Veterinary Microbiology 228 (2019) 101–111

Contents lists available at ScienceDirect

Veterinary Microbiology

journal homepage: www.elsevier.com/locate/vetmic

Duck innate immune responses to high and low pathogenicity H5 avian influenza viruses

Ximena Fleming-Canepa[a], Jerry R. Aldridge Jr.[c,d], Lauren Canniff[a], Michelle Kobewka[a], Elinor Jax[e], Robert G. Webster[c], Katharine E. Magor[a,b,*]

[a] Department of Biological Sciences, CW405 Biological Sciences Building, University of Alberta, Edmonton, Alberta, T6G 2E9, Canada
[b] Li Ka Shing Institute of Virology, University of Alberta, Edmonton, T6G 2E1, Canada
[c] Division of Virology, Department of Infectious Diseases, St. Jude Children's Research Hospital, Memphis, TN, 38105, USA
[d] Institute of Parasitology, McGill University, 21,111 Lakeshore Road, Ste-Anne-de-Bellevue, Quebec, H9X 3V9, Canada
[e] Department of Migration and Immuno-Ecology, Max Planck Institute for Ornithology, Radolfzell, 78315, Germany

ARTICLE INFO

Keywords:
Interferon response
RIG-I, MAVS signalling
Attenuation
Interferon stimulated genes

ABSTRACT

Ducks are the reservoir host of influenza A viruses, and are permissive for replication of most strains, yet can elicit robust innate immune responses to highly pathogenic strains. Tissue tropism and viral amino acid differences affect virulence, but we have limited knowledge about how viral differences influence the host innate immune response. Here we compare the innate immune response in Pekin ducks to a recombinant highly-pathogenic avian influenza (HPAI) H5N1 virus and a naturally arising attenuated variant of this strain that differs at one amino acid in polymerase A (T515A), as well as ducks infected with two different H5 strains of low pathogenic avian influenza (LPAI). Using qPCR we examined the relative abundance of transcripts for RIG-I and interferon-beta (IFNβ), and downstream interferon stimulated genes (ISGs). The polymerase PA (T515A) mutation did not significantly affect replication *in vivo* but greatly attenuated host interferon responses. ISG induction was robust for both H5N1 strains, but was three times lower for the PA mutant strain. Low pathogenic viruses elicited detectable induction of RIG-I, IFNβ and ISGs in lung and intestine tissues that correlated with the recovery of viruses from tracheal or cloacal swabs. Several genes in the MAVS signaling pathway were also upregulated by H5N1, which contributed to further amplification of the signal. We also examined hematoxylin-eosin stained tissue sections and observe evidence of lung pathology and splenocyte depletion with both H5N1 viruses at 3 dpi, and recovery by 6 dpi. However, for both H5N1 strains we observed inflammation around neurons in brain, with increased cytokine expression in some individuals. Our findings reveal HPAI H5N1 viruses induced stronger innate immune responses to the infection, while LPAI viruses elicit a milder response.

1. Introduction

Ducks are the natural reservoir, and often asymptomatic carriers of influenza A viruses (Kida et al., 1980; Webster et al., 1992). Even when infected with HPAI strains that are deadly to humans and chickens, ducks generally exhibit only mild symptoms of infection. Ducks contributed to the spread of H5N1 strains, which were lethal to chickens and humans, but of varying pathogenicity to ducks (Hulse-Post et al., 2005; Sturm-Ramirez et al., 2005). Some strains that emerged in 2004 killed ducks, but these viruses rapidly attenuated to become less pathogenic to ducks. This was observed in the laboratory during a duck challenge experiment with a HPAI H5N1 strain, A/Vietnam1203/04 (VN1203), where a small plaque-forming mutant arose that no longer killed ducks, but remained lethal to mice and ferrets (Hulse-Post et al., 2007). This small plaque-forming mutant contained five amino acid differences, which were each examined in more detail using site-directed mutagenesis of a reverse genetics version of VN1203 (rgVN1203). Of particular interest, the polymerase A T515A variant, no longer caused mortality in ducks, but remained lethal to mice, and ferrets. Intriguingly, the polymerase activity of the PA T515A variant was not statistically different from the wild type VN1203 in a luciferase reporter assay (Hulse-Post et al., 2007), which suggests that the PA T515A residue may not affect viral replication efficiency thus how this mutation affects virulence in ducks remains unclear.

To understand the mechanisms that contribute to pathogenicity in the host species, we seek to compare the innate immune response to

* Corresponding author at: Department of Biological Sciences, University of Alberta, CW 405 Biological Sciences, Edmonton, Alberta, T6G 2E9, Canada.
E-mail address: kmagor@ualberta.ca (K.E. Magor).

https://doi.org/10.1016/j.vetmic.2018.11.018
Received 5 June 2018; Received in revised form 16 November 2018; Accepted 16 November 2018

HPAI or LPAI viruses in ducks. RIG-I is the most important sensor of influenza virus (Kato et al., 2006), and we previously showed that RIG-I is upregulated during infection in ducks (Barber et al., 2010), but not present in chickens and this difference may contribute to why ducks suffer less pathology upon infection. In humans, the activation of RIG-I requires TRIM25-mediated polyubiquitination of lysine 172 in the second CARD domain (Gack et al., 2007). Recently, Zeng et al demonstrated that unanchored ubiquitins can also activate RIG-I (Zeng et al., 2010), suggesting that the role of TRIM25 may be to synthesize the K63-linked polyubiquitin chains (Jiang et al., 2012). We demonstrated that in ducks, TRIM25 attaches ubiquitin at different residues, but this attachment was not necessary for activation of duck RIG-I, because mutation of the lysine residues did not impair TRIM-mediated activation of duck RIG-I (Miranzo-Navarro and Magor, 2014). The crystal structure of RIG-I with bound ubiquitin chains resolved the controversy between models by suggesting that unanchored and anchored diubiquitin can interchangeably mediate the activation, through structural stabilization of the tetramer of CARD domains (Peisley et al., 2014). Apart from duck TRIM25, we do not know whether other postranslational modifiers of RLRs, or which components of the MAVS signalling pathway are present or functional in ducks.

RIG-I and MDA5 initiate signaling through MAVS leading to production of interferon and ISGs. Each protein encoded by the ISGs will target different steps of the viral life cycle, many of which interfere with viral replication (Schoggins et al., 2011). Key ISGs downstream of RIG-I signaling were defined in the mouse as the 'RIG-I bioset' by comparing gene expression upon influenza infection in wildtype and RIG-I knockout cells (Loo et al., 2008). Previously, we identified interferon-stimulated genes (*IFIT*, *OASL, ISG12* and *IFITM)* using subtractive hybridization to identify genes upregulated by influenza viruses. We showed that RIG-I and these ISGs were greatly upregulated by a HPAI strain, and only weakly upregulated in response to a LPAI strain (Barber et al., 2010; Vanderven et al., 2012). Here, we used the duck genome sequence (Huang et al., 2013) to identify the genes that encode proteins involved in the MAVS signaling pathway in the duck, and key ISGs defined as the RIG-I bioset, and examined their relative expression by qPCR at one to three days post infection with a recombinant version of the HPAI H5N1 virus A/Vietnam 1203/2004 (rgVN1203) or the polymerase A mutant of this virus (T515A), which is attenuated in ducks. We also compared immune responses to two LPAI H5 strains A/duck/British Columbia 500/2005 (H5N2) (BC500) and A/duck/British Columbia 544/2005 (H5N9). We measured gene expression in either lung or intestine, which are known to be the main sites of replication for these viruses (Sturm-Ramirez et al., 2004; Webster et al., 1978), and we also assessed the pathology caused by HPAI variants by histology and compared cytokine expression associated with pathogenicity.

2. Methods and materials

2.1. Viruses, infections and RNA extraction

RNA samples were obtained from tissues of ducks that were mock-treated, or infected with highly pathogenic avian influenza, or low pathogenic avian influenza as described in detail previously (Barber et al., 2010). Highly pathogenic rgA/Vietnam/1203/04 (H5N1) (rgVN1203) was made by reverse genetics (Salomon et al., 2006) and characterized as less pathogenic in ducks than the original virus (Marjuki et al., 2010), with an IVPI score of 1.76 compared 2.32 for wild type VN1203. During an infection of ducks with wildtype VN1203, five mutations arose naturally leading to large and small plaques of different pathogenicities, and each of these mutants was re-created in the recombinant rgVN1203 (Hulse-Post et al., 2007). The PA T515A strain did not kill ducks upon inoculation by the natural route, but killed 3/5 ducks when injected intravenously. By comparison, rgVN1203 killed 3/6 ducks when inoculated by the natural route, and 7/9 when injected intravenously. Low pathogenic A/mallard/BC/500/05 (H5N2) (BC500) and A/mallard/BC/544/2005 (H5N9) were isolated during surveillance of wild ducks in Canada.

Outbred 1 day-old White Pekin ducks were obtained from either Metzer Farm or Ideal Poultry and housed in-house until mature at 6 weeks. Adult ducks were infected with 10^6 EID_{50} of virus by the natural route or mock-infected with PBS-only. To compare infection with highly pathogenic viruses rgVN1203 and PA T515A, tracheal and cloacal swabs were taken. Neat swab material was injected into 3 eggs, incubated and tested for hemagglutination, and positive swab material was titred further by determining the EID_{50} in eggs (Reed and Muench, 1938). The titres of tracheal swabs taken at 3 dpi with rgVN1203 and PA T515A are not statistically different (Supplementary Fig. 1).

Highly pathogenic viruses caused signs of disease including cloudy eyes, loss of appetite and reduced mobility, and one duck displayed torticollis, but no ducks died. Low pathogenic viruses caused no signs of disease. All animal experiments were approved by the Animal Care and Use Committee of St. Jude Children's Research Hospital and performed in compliance with relevant institutional policies, National Institutes of Heath regulations and the Animal Welfare Act.

To examine the time course of infection with each low pathogenic virus, tracheal and cloacal swabs were taken each day and stored frozen. Neat swab material was inoculated in 3 eggs, and tested for hemagglutination. Swab material for BC500 was positive in cloaca but not trachea, and the EID_{50} was determined for swabs positive in 3 eggs. BC544 had some virus positive swabs for both trachea and cloaca at 2 dpi and 3 dpi, but these were not titred further because most were not positive in 3 eggs. Titres for tracheal or cloacal swabs for some ducks infected with rgVN1203 and BC500 and subtractive hybridization were reported previously (Vanderven et al., 2012), and RIG-I expression using ABI chemistry was reported previously (Barber et al., 2010).

Ducks were euthanized, tissue samples harvested, and total RNA extracted using TRIzol (Invitrogen). The RNA was DNase treated, and stored at −80 °C. Lung and spleen samples were collected from 3 ducks at each timepoint; 1dpi, 2dpi and 3 dpi with rgVN1203 and PA515 in two separate experiments (one week apart). Tissues were not taken from intestine, as cloacal swabs were mostly negative for these viruses. In a third experiment, lung, spleen, brain and bronchiol-alveolar-lavage (BAL) washes (n = 3) were collected at 3 dpi and 6 dpi with rgVN1203 or PA T515A. Lung, spleen and intestine samples were collected from 3 ducks at each timepoint for BC500, BC544 and mock-infected ducks. Tissues from a duck infected with rgVN1203 or PAT515A from each of the three experiments were collected at time of necropsy at 3 dpi or 6 dpi, fixed in 10% neutral buffered formalin, sectioned and stained with hematoxylin-eosin by the Veterinary Core Pathology Laboratory at St. Jude Children's Research Hospital. Pathology scoring of histological sections was done by Animal Pathology Services, Edmonton, Alberta, with identity of samples initially undisclosed, then later confirmed with identity disclosed.

2.2. Identification of MAVS pathway genes

We identified genes in the RIG-I pathway and downstream in the duck genome sequence available on PreEnsembl (http://pre.ensembl.org/Anas_platyrhynchos/Info/Index). Primers based on these sequences were used to amplify full or partial cDNA sequences, which were cloned and fully sequenced. cDNA sequences were deposited for duck MDA5 (GenBank ID: KF483837), duck *TRIM25* (Genbank ID: KF483852), *MAVS* (Genbank ID: KF483848); *RSAD2* (GenBank ID: KF483849). IRF7 (Genbank ID: KF483851) was identified by 5′ rapid amplification of cDNA ends (RACE) using gene specific primer (5′-GTG ACG GCG AAG ACC TTG TGA GGG TC-3′) and the BD SMART™ RACE cDNA Amplification Kit (Clontech). A putative sequence of RNF135 (GenBank ID: KF483850) (also called Riplet) was obtained by 5′ RACE using reverse primer (5′-GAG ATT GTG CTG GTT GGG AAC TGC TGA-3′) and cDNA template generated with a gene-specific primer (5′-CAG AAA GCA GGA TAA AGA GGA TTT G-3′) and the BD SMART™ RACE Kit

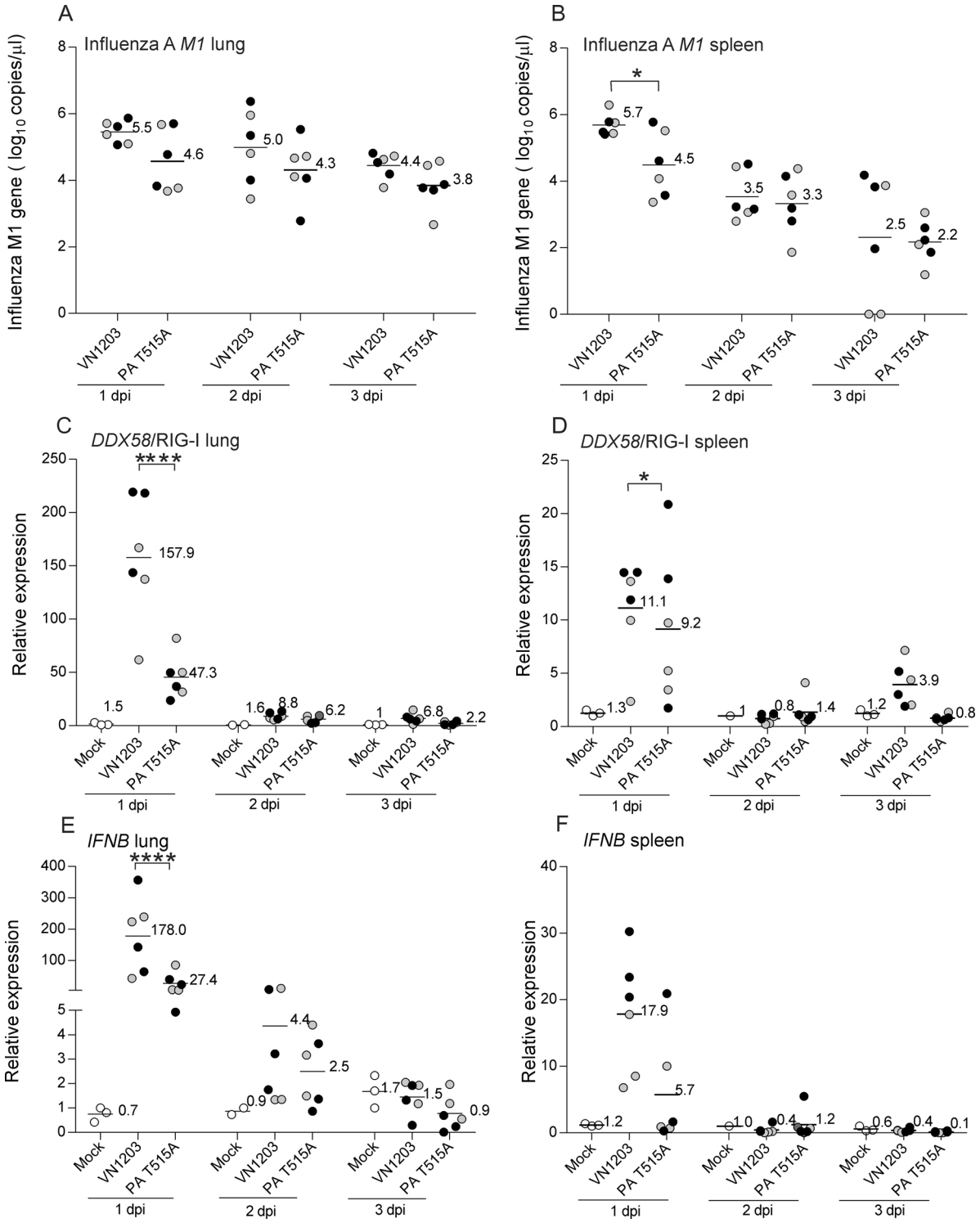

Fig. 1. Related H5N1 strains replicate in lung and spleen but elicit different IFN responses. H5N1 replication was determined by amplification of the influenza A matrix 1 gene (*M1*). RNA was extracted from lung and spleen tissues of ducks at 1, 2 or 3 dpi with rgVN1203 or the attenuated PA T515A viruses. Influenza matrix gene copy number is determined against a known copy number of an influenza matrix M1 clone. Fold expression of RIG-I (C and D) or *IFNB* (E and F) in duck lung and spleen following infection with rgVN1203 or PA T515A is shown relative to a mock treated duck. Each dot represents one duck and mean fold-induction is indicated for the ducks (n = 6). Dark circles (males) and light circles (females). Significant differences between rgVN1203 or PA T515A in mean viral titre or gene transcript levels on each day were determined by two-way ANOVA ($P < 0.05$) *$P < 0.05$, **$P < 0.01$, ****$P < 0.0001$. Non-significant differences are not indicated.

(Clontech). However, we are unable to recover a homologous exon 1. We recovered an alternate exon which is correctly spliced upstream of exon 2, and encodes an open reading frame in the correct frame. However, when the encoded amino acid sequence is aligned with vertebrate homologues it is clear that duck Riplet does not encode a RING domain. Attempts to amplify using primers that match the RING domain of zebrafinch and other species also failed to generate a product. We examined transcripts within RNAseq data (Huang et al., 2013), and it shows that many sequences align to this putative exon 1, confirming that it is expressed. The truncated gene was subsequently amplified

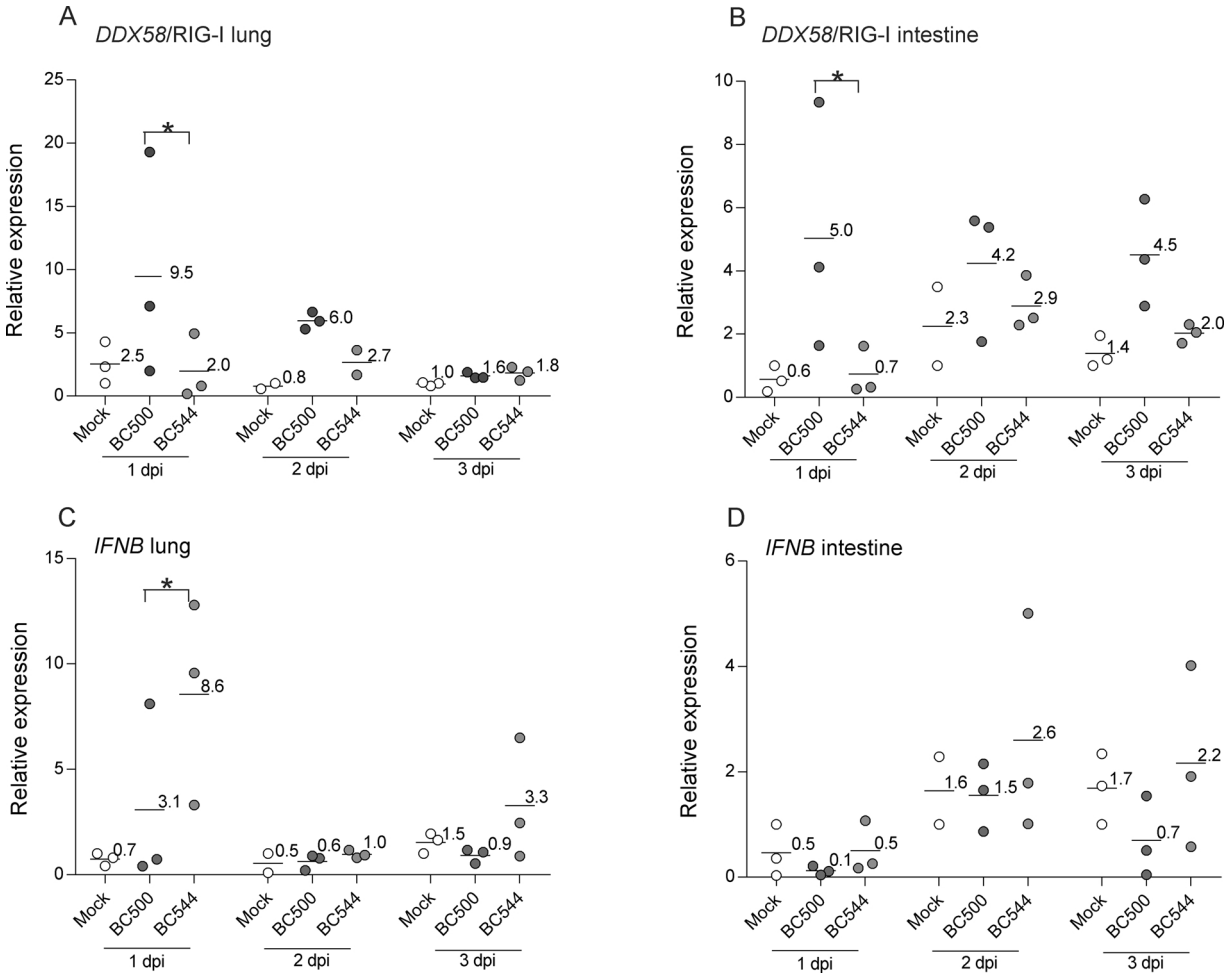

Fig. 2. Low pathogenic avian influenza strains slightly upregulate innate immunity in duck lung and intestine. RNA was extracted from duck lung or intestine tissues at 1, 2 and 3 dpi with indicated strains and gene expression relative to *GAPDH* was determined by qPCR. Fold expression of RIG-I and *IFNB* in lung (A and C) or intestine (B and D) tissues of ducks following infection with BC500 or BC544 from infected ducks (n = 3) relative to a mock-treated animal each day (each dot represents one duck). The mean fold induction is indicated with a line. Significant differences between isolates each day were determined by two-way ANOVA ($P < 0.05$). *$P < 0.05$, **$P < 0.01$.

using the following primers: 5′-ATG CTC AAA TGT GTC ACT TTA AAG GAG GAA C-3′ and 5′-GCT AAA CAC TGA AGC TGG CAT AGA AGC-3′ using KAPA High-Fidelity DNA Polymerase (KAPA Biosystems). We identified the duck homologues for three well-characterized interferon-stimulated genes, *MX1*, *PKR* and *RSAD2*. *RSAD2* is highly conserved with other species, although avian and mammalian viperin differ greatly in the N-terminal end. Complete cDNA sequences were not amplified for PKR or MxA, but sequences were assembled from the genome sequence. Duck PKR is lacking part of the second RNA binding domain, which may affect function.

2.3. Quantification of gene expression by qPCR amplification

To evaluate transcript abundance for genes in the RIG-I bioset in influenza-infected tissues we used qPCR using the 7500 Fast Real Time PCR instrument (Applied Biosystems) and the FastStart TaqMan® Probe Master mix (Roche). Primers and probe sets (Integrated DNA Technologies (IDT)) were designed using Primer Express version 3.012.5 or IDT Primer Quest (Supplementary Table 1). Quantitative PCR primers and probes for *DDX58* (RIG-I), *IFNB*, *IFNG*, *IL6*, *OASL*, *IFIT5* and *MX* have been described previously (Saito et al., 2018), and *IFITM3* (Blyth et al., 2015). Absolute quantification of influenza matrix 1 (M1) gene was done as described previously (Saito et al., 2018). Transcripts for low pathogenic viruses were below the limit of detection in mRNA prepared from lung or intestinal tissue.

qPCR amplifications were done using cDNA for mock infected or influenza-infected lung tissues. PCR conditions were 95 °C for 10 min, and 40 cycles of denaturation at 95 °C for 15 s followed by annealing-extension at 60 °C for 1 min. All samples were run in triplicate, and each assay repeated at least once. Target genes were normalized to the housekeeping gene GAPDH using the relative quantitation method (ΔΔCT), and the 7500 Fast system software version 1.4 (Applied Biosystems). To show gene expression for each individual duck since each infection is unique, the relative expression is shown in comparison to one mock-infected animal. Heat maps were generated using the mean of fold upregulation of each gene normalized to GAPDH for infected ducks, compared to the mean of mock-treated ducks.

2.4. Statistical analyses

All samples at 1 dpi were statistically different from mock-treated animals, which can be readily observed, so bars indicating significance were omitted for clarity. For statistical power, the data from two experiments are combined for analysis. Analysis of variance was done using a two-way ANOVA, and a post hoc Tukey multiple comparisons test to compare the mean value of each treatment. Only statistically significant differences between infections being compared at each time point are indicated.

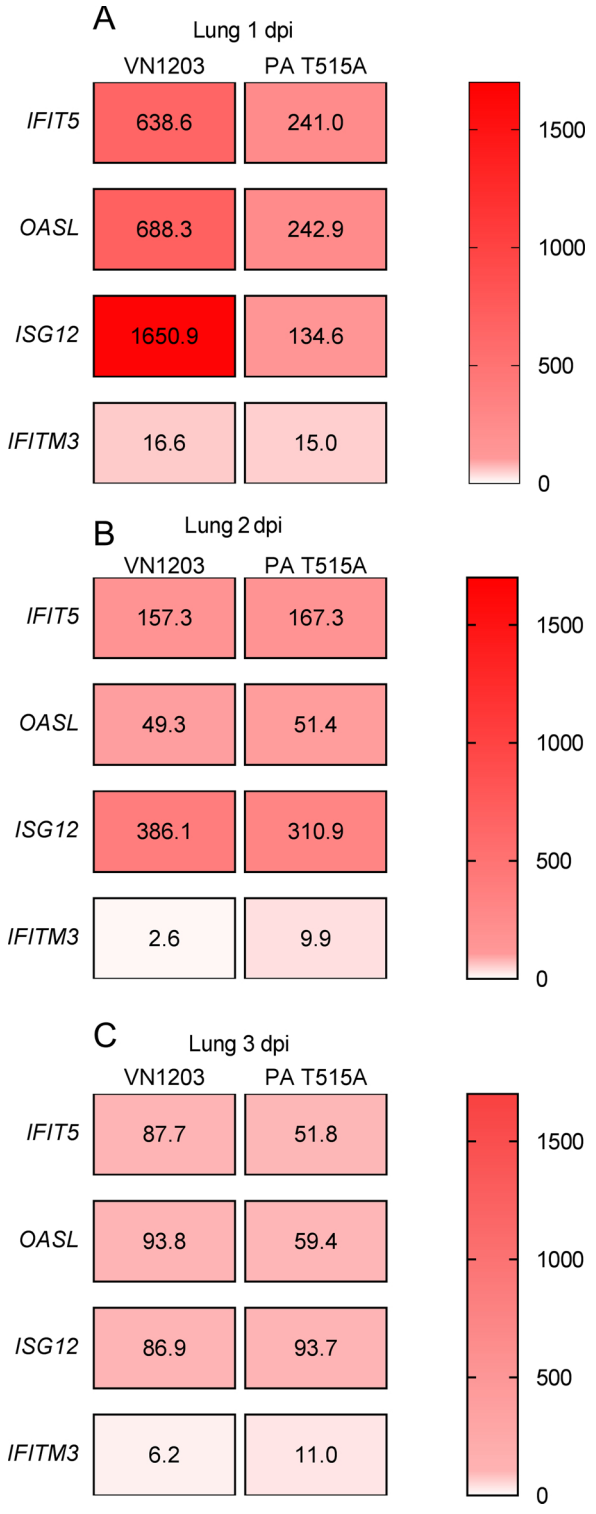

Fig. 3. ISGs are induced in lung by highly pathogenic viruses. Heat maps were created from average fold-induction of ISGs relative to GAPDH in tissues isolated from ducks infected with highly pathogenic viruses compared to mock-treated ducks. qPCR was carried out for *IFIT5*, *OASL*, *ISG12* and *IFITM3* from mRNA isolated from lung tissue (n = 6) taken at 1, 2, and 3 dpi with rgVN1203 or PA T515A (A–C).

3. Results

3.1. Highly pathogenic avian influenza strains rgVN1203 and attenuated variant PA T515A replicate similarly but elicit different interferon responses

We performed infections of White Pekin ducks by the natural route using two highly related viruses, a recombinant version of the HPAI strain A/Viet Nam 1203/2004 (rgVN1203) and a mutant created in the same backbone, bearing a single mutation in the polymerase A gene, PA T515A. This mutation arose naturally in the wild type VN1203 viral isolate, and the mutant was characterized as less pathogenic to ducks (Hulse-Post et al., 2007). We compared the level of viral infection and systemic spread in tissues by quantifying the expression of the influenza matrix gene (M) in lung (Fig. 1A) and spleen tissues (Fig. 1B). For rgVN1203 and PA T515A, a similar level of virus replication was seen in lung tissue over 3 days, with the PA mutant demonstrating slightly lower influenza M transcript levels, although the difference was not statistically significant; however, the PA T515A mutant demonstrated significantly less systemic spread to spleen as compared to the parental virus at 1 dpi.

RIG-I is highly upregulated by infection with rgVN1203, but only weakly by BC500 (Barber et al., 2010), suggesting that the interferon produced is related to the virulence of the strain. To compare the innate immune response to these nearly identical H5N1 viruses, we examined the expression of *DDX58* (RIG-I) and *IFNB* following infection. We compared the relative expression of *DDX58* (RIG-I) in tissues obtained from ducks either mock-treated, or infected with rgVN1203 or the PA T515A variant. The relative abundance of duck *DDX58* transcripts in lung tissue was increased 157-fold at 1 day post infection (dpi) in ducks infected with rgVN1203, but only 47.3 fold in ducks infected with PA T515A, relative to mock-infected animals (Fig. 1C). The difference in relative expression of RIG-I in spleen was less than in lung between the two virus strains, yet expression induced by PA T515A remained significantly less than that induced by rgVN1203 (Fig. 1D). The relative abundance of *IFNB* transcripts increased by 178-fold in lung tissue at 1 dpi with rgVN1203 compared to 27-fold for the PA T515A mutant, and this expression was greatly decreased by 2 dpi (Fig. 1E). *IFNB* expression in spleen was induced by both rgVN1203 and PA T515A (Fig. 1F). The replication of rgVN1203 and PA T515A viruses was not statistically different in tissues examined, however the expression of innate immune genes in response to the attenuated PA T515A strain were much lower.

3.2. RIG-I (DDX58) and IFNB are weakly upregulated in lung or intestine by low pathogenic viruses

We also performed infections with two LPAI strains that were isolated from ducks during environmental screening in British Columbia, Canada, an H5N2 A/mallard/BC500/2005 (BC500) and an H5N9 A/mallard/BC544/2005 (BC544). Both strains replicated in ducks and were recovered in cloacal and tracheal swabs. Viral matrix gene transcripts in tissues were below the level of detection, as is expected for LPAI viruses. We compared innate responses by examining the expression of *DDX58* (RIG-I) and *IFNB* by qPCR following infection. After normalizing to the housekeeping gene *GAPDH*, we found that *DDX58* transcripts were more abundant in lung tissue at 1 and 2 dpi with BC500, compared to BC544 (Fig. 2A). Similarly, in intestine tissue, *DDX58* expression was higher in response to infection with BC500 throughout all 3 dpi (Fig. 2B). *IFNB* transcripts were higher for BC544 in lung, than BC500 (Fig. 2C), while *IFNB* was higher for some individual ducks infected with BC544 at 2 and 3 dpi (Fig. 2D). The induction of innate responses as indicated by expression of RIG-I and *IFNB*, showed the response to both LPAI viruses was weak, and these IFN responses in lung or intestine tissue correlated with virus recovery of from either tracheal or cloacal swabs, respectively.

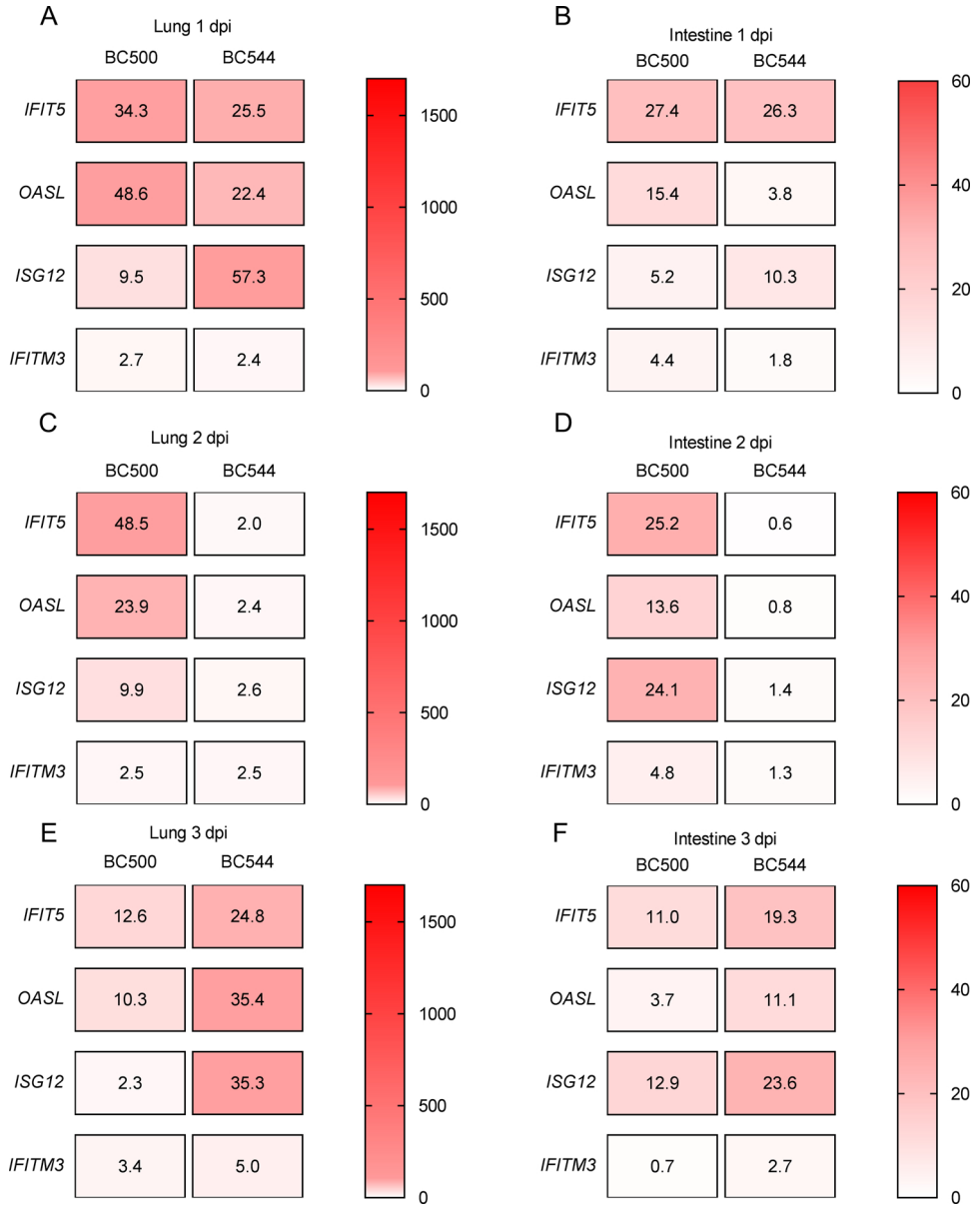

Fig. 4. ISGs are induced in lung and intestine by low pathogenic viruses. Heat maps were created from average fold-induction of ISGs relative to GAPDH in tissues obtained from ducks infected with low pathogenic viruses compared to mock-treated ducks. qPCR was carried out for *IFIT5*, *OASL*, *ISG12* and *IFITM3* from mRNA isolated from lung (A, C, E) or intestine (B, D, F) tissue taken at 1, 2, and 3 dpi with BC500 or BC544 (n = 3).

3.3. ISGs are upregulated in the primary sites of replication

To determine whether the host responses downstream of RIG-I were similar following infection with these viruses, we compared the expression of four ISGs in response to HPAI viruses in lung, or LPAI strains in lung and intestine. The ISGs examined were previously discovered using subtractive hybridization and were found to be highly expressed in response to rgVN1203 (Vanderven et al., 2012). We compared transcript abundance by qPCR at 1, 2 and 3 dpi, and while the level of induction was variable for each gene, the response to rgVN1203 was at least 3 times higher than the response to the mutant PA T515A at 1 dpi (Fig. 3A), and expression of all genes similarly declined for both rgVN1203 and PA T515A at 2 dpi and 3 dpi (Fig. 3B and C). We found that ISGs were expressed at higher levels in response to rgVN1203 as compared to PA T515A at 1 dpi, which correlates positively with their known pathogenicity. Thus the overall interferon response to the PA mutant was much lower than to the rgVN1203 virus.

Expression of ISGs was induced by infection with the LPAI strains BC500 and BC544 in the lung at 1, 2 and 3 dpi. ISGs in lung were upregulated at 1 and 2dpi in response to BC500, and days 1 and 3 for BC-544 (Fig. 4A, C and E). In intestine, ISG expression was increased at 1, 2 and 3 dpi for all genes by BC500, but only on days 1 and 3 following infection for BC544 (Fig. 4B, D and F). The expression of most genes examined decreased by day 3 following infection with BC500. The expression profile for ISGs stimulated by BC544 being higher at 1 dpi and 3 dpi correlates with the viral load inoculated *via* the trachea, and replication at 3 dpi. Overall, the induction of ISGs by LPAI viruses reflects the tissue tropism of the virus.

3.4. MAVS signaling pathway genes are upregulated by rgVN1203

To determine whether the MAVS signaling pathway is upregulated during infection with influenza virus in ducks, we compared the expression of components of this pathway by qPCR in rgVN1203-infected lung and BC500-infected lung and intestine samples. Because peak RIG-I expression was evident at 1 dpi for each virus, we examined

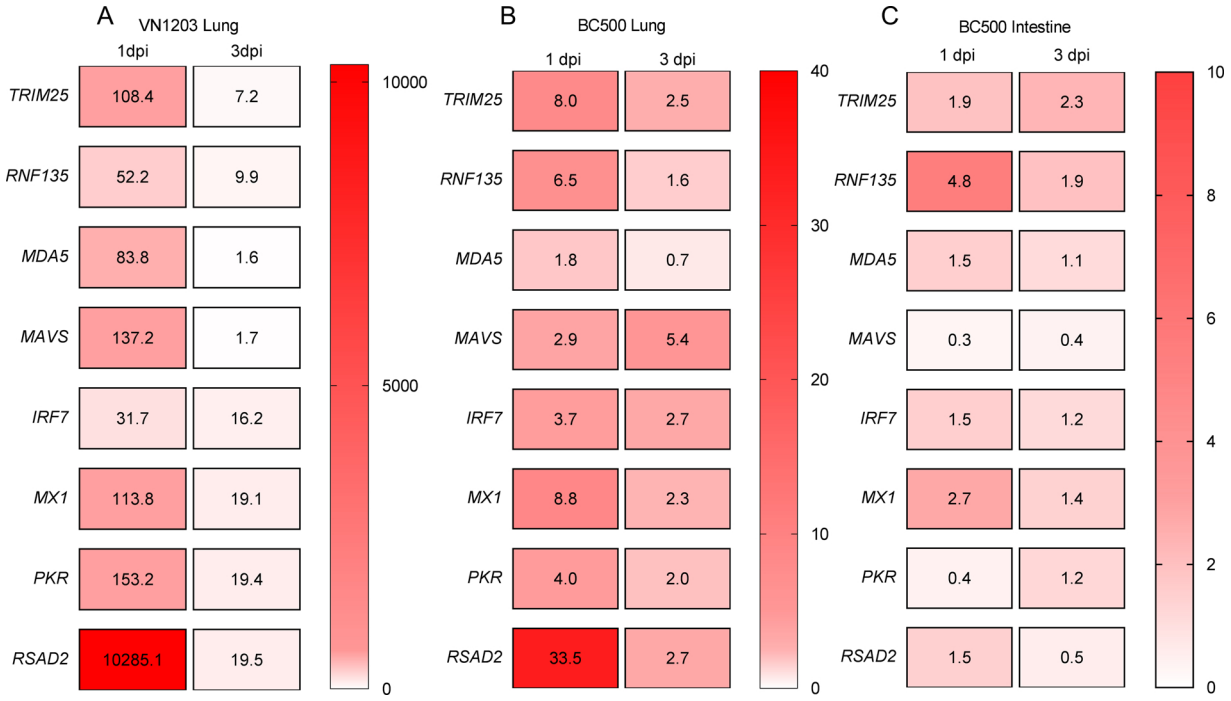

Fig. 5. RLR pathway genes are upregulated in lung and intestine of influenza A infected ducks. Heat maps showing fold induction of mRNA transcripts for RLR pathway genes at 1 and 3 dpi with rgVN1203 in lung (A) lung or BC500 in lung (B) or intestine (C) relative to a mock infected animal each day (n = 3).

expression only at 1 and 3 dpi. Transcript abundance was increased for *TRIM25, RNF135, MDA5, MAVS* in lung tissue by infection with rgVN1203 at 1 dpi but has decreased by 3 dpi (Fig. 5A). Similarly, these genes were induced in lung tissue at 1 dpi with BC500 (Fig. 5B) and slightly increased in intestine tissue at 1 dpi with BC500 (Fig. 5C). Transcript abundance of *IRF7* is induced by rgVN1203 infection, and remained high from 1 to 3 dpi. IRF7 increased by 32-fold at 1 dpi and 16-fold at 3 dpi with rgVN1203, but only 4-fold by BC500 in lung and not significantly induced in intestine as compared to untreated controls. To examine the magnitude of the response we examined three well characterized ISGs, including *MX1*, *PKR* and *RSAD2*, which are induced in lung tissue of ducks by 113-fold, 153-fold and 10285-fold at 1 dpi with VN1203, all returning to 19-fold by 3 dpi. These ISGs are upregulated by BC500, 8-fold, 4-fold and 34-fold in lung, and less in intestine.

3.5. H5N1 viruses show similar replication but differ in viral spread

To examine the extent of spread of rgVN1203 and PA T515A in tissues of infected ducks over a longer time, tissue samples were collected at 3 dpi and 6 dpi. Virus replication was measured by qPCR quantification of the influenza matrix gene. Both rgVN1203 and PA T515A replicated to similar levels by 3 dpi as indicated by a similar virus load in bronchial-alveolar lavage fluid and lung tissue (Fig. 6A), but transcript levels in brain was lower on day 3 after infection with the PA variant strain compared to rgVN1203. Infection was cleared in lung and spleen by 6 dpi, but the virus load remained high in the brain of all three rgVN1203-infected ducks at 6 dpi, whereas only one PA T515A infected duck displayed a high titre (Fig. 6B). In most cases, the spread of rgVN1203 within infected individuals was greater in ducks as compared to the PA T515A variant.

To assess pathogenicity of rgVN1203 and PA T515A we examined the expression of two genes often associated with pathogenicity, *IL6* and *IFNG*. IL-6 was elevated in the brain of one duck infected with VN1203 at 3 dpi (Fig. 6C), and one duck infected with PA T515A at 6 dpi (Fig. 6D). *INFG* was upregulated in lungs of all ducks at 3 dpi, and the brain of one duck at 3 dpi and 6 dpi infected with VN1203 (Fig. 6E and F). Combined, these data suggest that ducks resolve both infections over time and that the cytokine expression profiles of ducks suggest that although most individuals recover, some show signs that may be associated with pathology.

To assess the extent of damage due to infection with highly pathogenic avian influenza, we fixed tissues from ducks from each of the three experiments with rgVN1203 and PA T515A. Tissues were mounted, sectioned and stained with hematoxylin and eosin (Fig. 7). Pathology was initially scored blind for all sections, and confirmed later upon disclosure of identity (Supplementary Table 4). Histology of lung tissues at 3 dpi with rgVN1203 revealed sporadic, small lymphoid follicles and localized areas of inflammation centered on airways with accumulation of leukocytes extravasating blood vessels (Fig. 7A). The spleen of this duck appeared surprisingly normal (Fig. 7B) and viral load was undetectable in this tissue. In the other two individuals, splenic involvement indicated a systemic infection and showed mild depletion of periarterial areas at 3 dpi with rgVN1203 (Supplementary Table 2) similar to that observed for PA T515A (Fig. 7E). The brain appeared mostly normal at 3 dpi with rgVN1203 with a few knots of mononuclear cells (Fig. 7C), while inflammation and cell clusters around neurons were seen in the brain of one of the ducks infected with PA T515A (Fig. 7F). By 6 dpi, both lung and spleen of rgVN1203 and PA T515A were on their way to recovery, with normal airways and follicles evident in lung (Fig. 7G and J) and spleens less depleted of leukocytes (Fig. 7H and K). Brains of ducks infected with both rgVN1203 and PA T515A showed inflammation and cell clusters around neurons with evidence of some perivascular reaction (Fig. 7F, I and L). Overall, tissues from ducks infected with either of the H5N1 variants showed areas of inflammation in the lung, evidence of splenic involvement, and virus spread to the brain. At 6 dpi the virus was not detected in the lung or spleen, which showed evidence of recovery, although some pathology was evident in the brains following infection with either virus strain.

4. Discussion

Here we compare the innate immune response in Pekin ducks to a recombinant H5N1 virus, rgVN1203 and an attenuated mutant of this

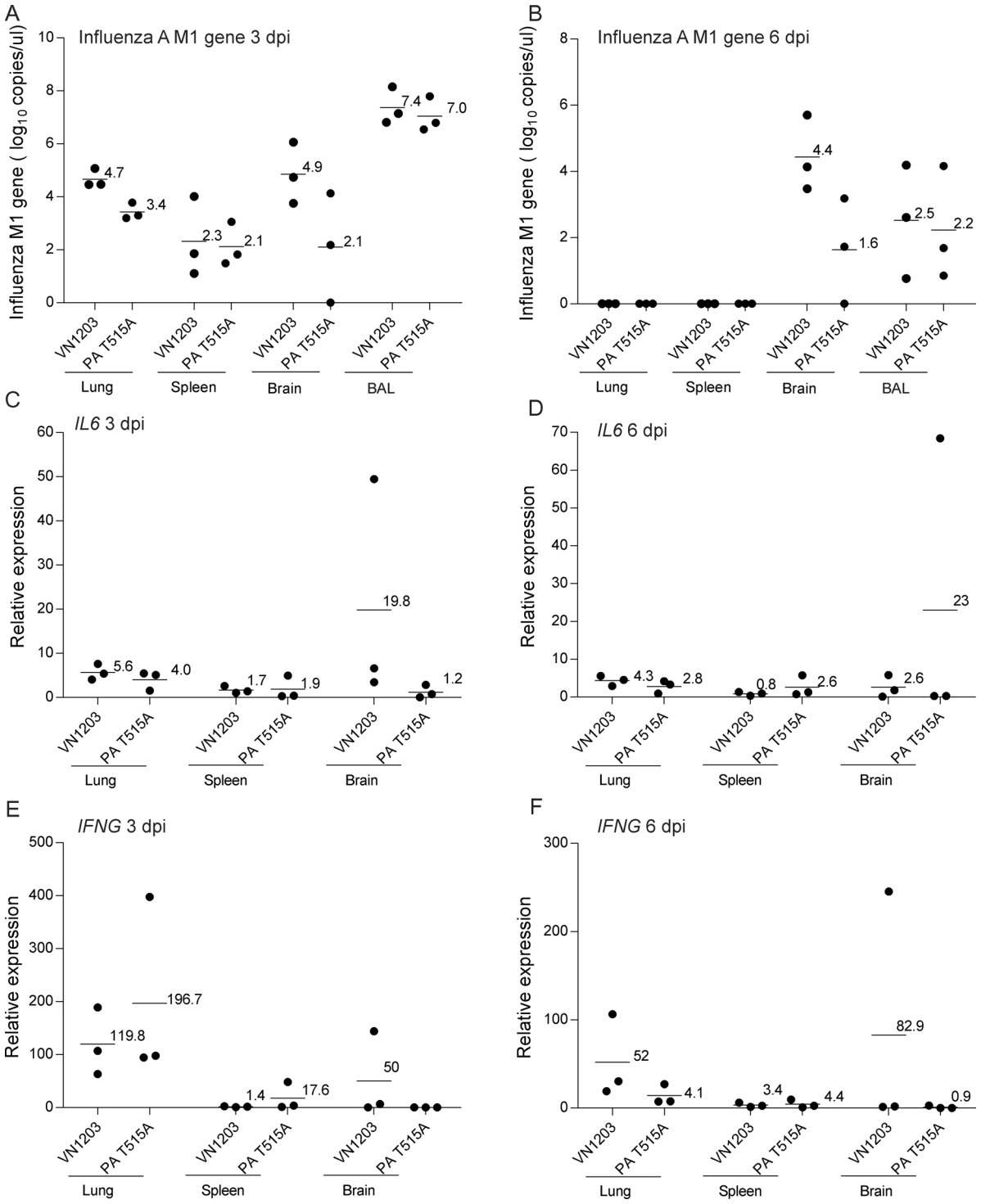

Fig. 6. Both H5N1 strains are cleared over time with some individuals showing high cytokine responses. H5N1 replication was determined by amplification of the influenza A matrix 1 gene (*M1*). RNA was extracted from lung, spleen and brain tissues and bronchio-alveolar lavage of ducks at 3 or 6 dpi with rgVN1203 or the attenuated PA T515A viruses. Influenza matrix gene copy number is determined against a known copy number of an influenza matrix M1 clone. Fold expression of *IL6* (C and D) or *IFNG* (E and F) in duck tissues following infection with rgVN1203 or PA T515A is shown relative to a mock treated duck. Each dot represents one duck (n = 3).

strain with a single mutation in PA, T515A. We also compare the immune gene expression in response to two low pathogenic strains, BC500 and BC544. Overall, the induction of immune genes, interferon B expression, and ISGs downstream correlates with viral load and virulence of these viruses. Previously, we showed that RIG-I was induced by rgVN1203 and BC500 (Barber et al., 2010), as well as downstream ISGs (Vanderven et al., 2012). Higher RIG-I expression correlated with H5N1 viruses of higher pathogenicity and replication in Muscovy ducks (Wei et al., 2013). We showed RIG-I and IFN responses were higher in response to the more pathogenic H5N1 virus in Pekin ducks, even though replication was similar (Saito et al., 2018). RIG-I induction increases with the age of duck (higher at 5 wk than 2 wk) and depends on strain of highly pathogenic virus (Pantin-Jackwood et al., 2012), and species of duck (Cagle et al., 2012), with a stronger innate response correlating

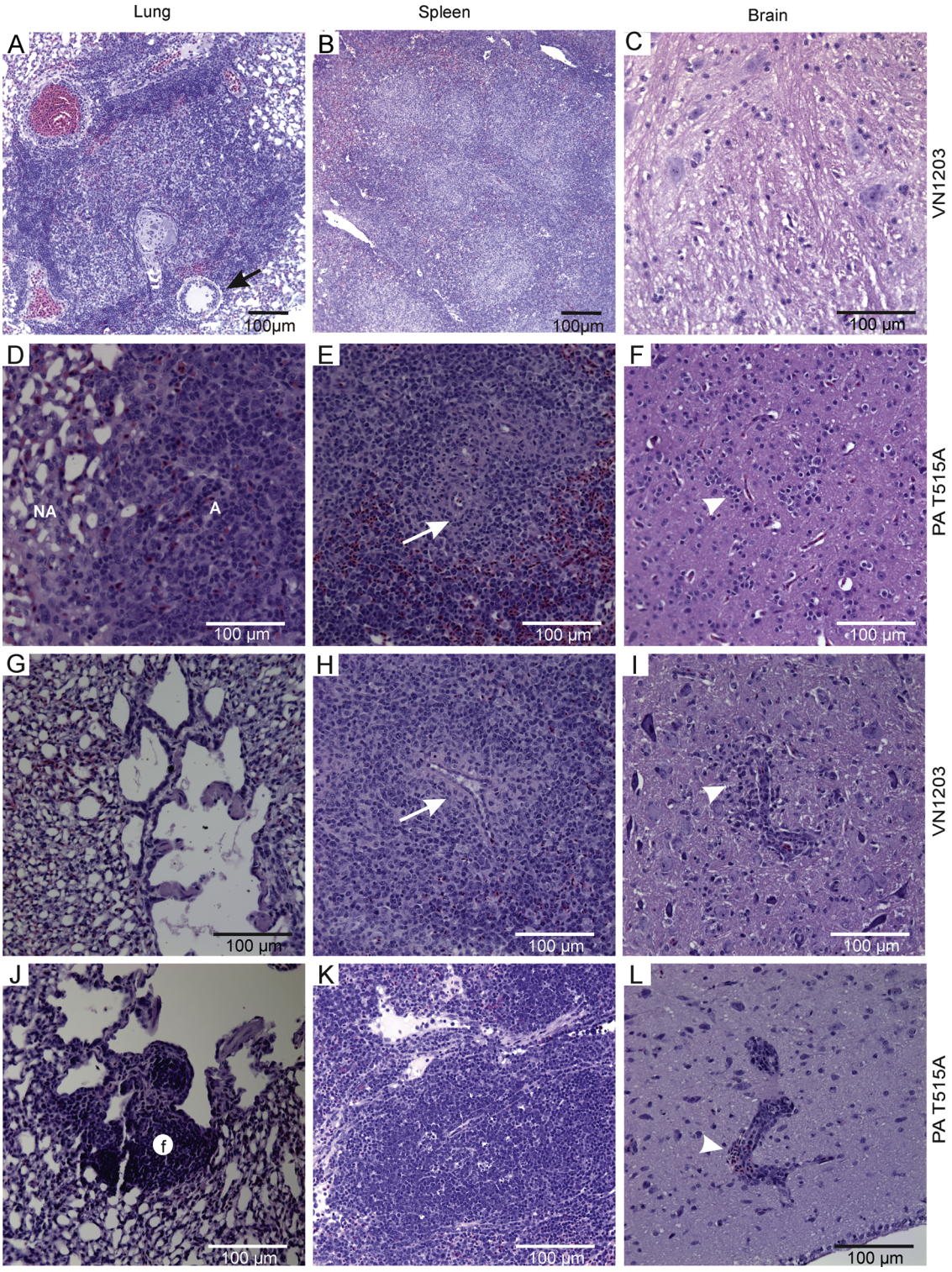

Fig. 7. Tissues of ducks infected with VN1203 and PA T515A show mild pathology and evidence of recovery. Light micrographs of hematoxylin and eosin stained sections of lung, spleen and brain tissue of ducks taken at 3 dpi with rgVN1203 (A–C) or PA T515 A (D–F) or 6 dpi with rgVN1203 (G–I) or PA T515 A (J–K). (A) Lung tissue shows lobular areas of inflammation and pavementing of leukocytes in blood vessel (black arrow). Lung tissue can show areas that are both affected (A) and not affected (NA) (D). A leukocyte accumulation or follicle (f) is apparent in recovering lung tissue (*J*). White arrows in spleen sections (E) indicate leukocyte depletion near vessels which is less evident by 6 dpi, suggesting recovery (H, K). White arrowheads in brain sections (F, I, L) indicate inflammation around clusters of neurons and evidence of perivascular reaction.

with a better outcome. Here, both HPAI strains induce a rapid and robust upregulation of innate signaling pathway genes in ducks, while LPAI strains only weakly induce these genes.

RIG-I is induced by rgVN1203 about three times higher than by the attenuated T515A variant. Further, IFNβ and downstream ISGs are upregulated much less by the PA T515A mutant than rgVN1203. The T515A variant arose naturally and reduced the virulence of the original isolate in ducks, but not in ferrets or mice (Hulse-Post et al., 2007). The PA T515A residue lies within a loop near the putative RNA binding groove and a channel of unknown function (He et al., 2008). Mutation

of residues within a region from residues 497–518, including the double mutant T515A, D516, highlighted a part of PA involved in infectivity, distinct from replication (Liang et al., 2012). How a mutation in this region can also affect interferon production is unclear. In the mouse, the bulk of the IFN-beta produced early in the response is made by epithelial cells, and later by myeloid cells (Kallfass et al., 2013). Barclay and co-workers recently showed that differences in ability to replicate in myeloid cells affected the production of interferon, and this required functional MAVS (Li et al., 2018). Mutations in polymerases, such as the avian PB2 variant E627, reduced viral replication in myeloid cells and consequent interferon production in mice, which was previously also seen in infection of human macrophages with recombinant viruses with polymerase genes from VN1203 (Mok et al., 2009). Similarly, differences in cytokine production upon infection of human macrophages by H5N1 variants correlated with differences in PA (Sakabe et al., 2013). Notably, the dysregulation of polymerases and subsequent production of short abberant RNAs, or mini-viral genomes, were recently shown to be the main agonists for RIG-I leading to production of interferon (Te Velthuis et al., 2018). It is plausible that mammalian residues in VN1203, such as the PB2 K627, similarly results in destabilization and production of mini viral genomes in avian hosts, and this is altered by the presence of PA T515A. Alternatively this residue affects replication in interferon-producing myeloid cells in the duck, which may also affect dissemination to distal tissues. It is particularly intriguing that the PA T515A mutation attenuates this virus only in ducks, but not ferrets or mice. We note that this is a rare mutation, not otherwise seen in nature.

The upregulation of RIG-I and *IFNB* was much less for BC500 and BC544 than for the HPAI viruses. BC544 replicated in both lung and intestine, albeit with a low titre present in both tracheal and cloacal swabs, and consequently only slightly induced innate immune genes in either tissue. However, BC500 also elicited only a weak innate response and we know that BC500 replicated well, as we recovered virus in cloacal swabs at titres of 10^4-10^7 EID_{50}. Nonetheless, amplification of matrix gene from the tissues taken from ducks infected with either LPAI virus was at the limit of detection, even when using ten times more template. Thus, the weak induction of ISGs that we observe reflects what is seen for whole tissue sample, which was taken closer to the jejeunal end, and individual cells may show a much greater response. BC500 was recovered by egg inoculation from duck ileum at $10^{3.0}$ to $10^{6.75}$ EID_{50} in a previous study (Smith et al., 2015). Older work showed titres of 3.8 to 7.8 EID_{50} in mucosal scrapings of small intestine from duodenal and cecal ends, respectively (Webster et al., 1978), and only sporadic cells of upper small intestine were shown to be involved in viral replication (Slemons and Easterday, 1978). Others have similarly shown only modest upregulation of innate immunity by other LPAI strains in duck intestine (Helin et al., 2018), spleen (Maughan et al., 2013) or isolated PBMCs (Adams et al., 2009).

We identified the genes involved in RLR signaling in ducks, and examined their gene expression by qPCR. The transcriptional profile of RIG-I and associated genes suggests a rapid induction of this pathway upon infection with HPAI rgVN1203, and much less by LPAI BC500. TRIM25, MAVS and IRF7 are all upregulated by rgVN1203. We previously showed that overexpression of duck MAVS-CARD initiates signaling by helical filament assembly and activates an IFNβ reporter (Wu et al., 2014). Since we have shown previously that RIG-I, TRIM25, and MAVS are functional, the induction of the MAVS signaling components is expected to contribute to amplification of the innate response to HPAI. In ducks, IRF7 is upregulated by interferon, and likely fulfills the role of IRF3. Finally, we see induction of many antiviral effectors downstream of the RIG-I pathway, including viperin, MX and PKR. These effectors, in addition to OASL, IFIT, and IFITM (Vanderven et al., 2012), are signatures of the response to a highly pathogenic avian influenza. It is important to note that the peak of the response was at 1 dpi with high ISG expression, and these genes are almost at normal levels by 3 dpi. Of note, all of these effectors are absent in the response to influenza infection in MEFs from the RIG-I knockout mouse (Loo et al., 2008). Here we show upregulation of the sensors and mediators of the RIG-I pathway by HPAI, demonstrating that gene expression of all components of the pathway are increased, most likely resulting in amplification of the response.

Histological examination of tissues shows evidence of mild pathology for both H5N1 strains, which is expected, since rgVN1203 is also attenuated compared to wild type VN1203. Pathology for both viruses appears as localized inflammation in the lung, depletion of leukocytes in the spleen, and evidence of lesions in the brain. Overall, the damage appears slightly more severe for the attenuated strain PA T515A, which may be a consequence of the lower immune response to this strain, or the animals randomly selected for histology. High cytokine responses in brains at 6 dpi were observed for some individual ducks, with rgVN1203 having one individual showing high *IFNG*, and one PA T515A infected duck showing high *IL6*. Although we cannot exclude the possibility that these individual ducks could be outliers, these results could be consistent with the pathology caused by these viruses. Histology of these brains reveals some pathology in each duck, including clusters of cells around neurons and evidence of perivascular reaction. Although there is significant variation between individuals and tissues examined, the ducks had cleared the viruses by day 6 in lung and spleen, and thus immune responses appear to be successful.

Acknowledgements

We thank J. Pasick (at National Center for Foreign Animal Disease) for sharing influenza strains A/mallard/British Columbia 500/2005 (H5N2) and A/mallard/British Columbia 544/2005 (H5N9). We also thank Patrick N. Nation, DVM, MVSc, PhD for blinded scoring of pathology from tissue histology. We thank John Franks and Patrick Seiler for help in BL3. This research was supported by the Canadian Institutes of Health Research grants MOP93561 and MOP125865 to KEM. Duck infections and isolation of infected tissues were conducted in Memphis and were supported by the National Institute of Allergy and Infectious Diseases, National Institute of Health under Contract No. HHSN27220140006C and by the American Lebanese-Syrian Associated Charities (ALSAC) to RGW.

Appendix A. Supplementary data

Supplementary material related to this article can be found, in the online version, at doi:https://doi.org/10.1016/j.vetmic.2018.11.018.

References

Adams, S.C., Xing, Z., Li, J., Cardona, C.J., 2009. Immune-related gene expression in response to H11N9 low pathogenic avian influenza virus infection in chicken and Pekin duck peripheral blood mononuclear cells. Mol. Immunol. 46, 1744–1749.

Barber, M.R.W., Aldridge Jr, J.R., Webster, R.G., Magor, K.E., 2010. Association of RIG-I with innate immunity of ducks to influenza. Proc. Natl. Acad. Sci. U. S. A. 107, 5913–5918.

Blyth, G.A., Chan, W.F., Webster, R.G., Magor, K.E., 2015. Duck interferon-inducible transmembrane protein 3 mediates restriction of influenza viruses. J. Virol. 90, 103–116.

Cagle, C., Wasilenko, J., Adams, S.C., Cardona, C.J., To, T.L., Nguyen, T., Spackman, E., Suarez, D.L., Smith, D., Shepherd, E., Roth, J., Pantin-Jackwood, M.J., 2012. Differences in pathogenicity, response to vaccination, and innate immune responses in different types of ducks infected with a virulent H5N1 highly pathogenic avian influenza virus from Vietnam. Avian Dis. 56, 479–487.

Gack, M.U., Shin, Y.C., Joo, C.H., Urano, T., Liang, C., Sun, L., Takeuchi, O., Akira, S., Chen, Z., Inoue, S., Jung, J.U., 2007. TRIM25 RING-finger E3 ubiquitin ligase is essential for RIG-I-mediated antiviral activity. Nature 446, 916–920.

He, Xiaojing, Zhou, Jie, Bartlam, Mark, Zhang, Rongguang, Ma, Jianyuan, Lou, Zhiyong, Li, Xuemei, Li, Jingjing, Joachimiak, Andrzej, Zeng, Zonghao, Ge, Ruowen, Rao, Zihe, Liu, Yingfang, 2008. Crystal structure of the polymerase PAC?PB1N complex from an avian influenza H5N1 virus. Nature Vol. 454, 1123–1126 (28 August 2008).

Helin, A.S., Wille, M., Atterby, C., Jarhult, J.D., Waldenstrom, J., Chapman, J.R., 2018. A rapid and transient innate immune response to avian influenza infection in mallards. Mol. Immunol. 95, 64–72.

Huang, Y., Li, Y., Burt, D.W., Chen, H., Zhang, Y., Qian, W., Kim, H., Gan, S., Zhao, Y., Li, J., Yi, K., Feng, H., Zhu, P., Li, B., Liu, Q., Fairley, S., Magor, K.E., Du, Z., Hu, X., Goodman, L., Tafer, H., Vignal, A., Lee, T., Kim, K.W., Sheng, Z., An, Y., Searle, S.,

Herrero, J., Groenen, M.A., Crooijmans, R.P., Faraut, T., Cai, Q., Webster, R.G., Aldridge, J.R., Warren, W.C., Bartschat, S., Kehr, S., Marz, M., Stadler, P.F., Smith, J., Kraus, R.H., Zhao, Y., Ren, L., Fei, J., Morisson, M., Kaiser, P., Griffin, D.K., Rao, M., Pitel, F., Wang, J., Li, N., 2013. The duck genome and transcriptome provide insight into an avian influenza virus reservoir species. Nat. Genet. 45, 776–783.

Hulse-Post, D.J., Franks, J., Boyd, K., Salomon, R., Hoffmann, E., Yen, H.L., Webby, R.J., Walker, D., Nguyen, T.D., Webster, R.G., 2007. Molecular changes in the polymerase genes (PA and PB1) associated with high pathogenicity of H5N1 influenza virus in mallard ducks. J. Virol. 81, 8515–8524.

Hulse-Post, D.J., Sturm-Ramirez, K.M., Humberd, J., Seiler, P., Govorkova, E.A., Krauss, S., Scholtissek, C., Puthavathana, P., Buranathai, C., Nguyen, T.D., Long, H.T., Naipospos, T.S., Chen, H., Ellis, T.M., Guan, Y., Peiris, J.S., Webster, R.G., 2005. Role of domestic ducks in the propagation and biological evolution of highly pathogenic H5N1 influenza viruses in Asia. Proc. Natl. Acad. Sci U. S. A. 102, 10682–10687.

Jiang, X., Kinch, L.N., Brautigam, C.A., Chen, X., Du, F., Grishinm, N.V., Chen, Z.J., 2012. Ubiquitin-induced oligomerization of the RNA sensors RIG-I and MDA5 activates antiviral immune response. Immunity 36, 959–973.

Kallfass, C., Lienenklaus, S., Weiss, S., Staeheli, P., 2013. Visualizing the beta interferon response in mice during infection with influenza A viruses expressing or lacking nonstructural protein 1. J. Virol. 87, 6925–6930.

Kato, H., Takeuchi, O., Sato, S., Yoneyama, M., Yamamoto, M., Matsui, K., Uematsu, S., Jung, A., Kawai, T., Ishii, K.J., Yamaguchi, O., Otsu, K., Tsujimura, T., Koh, C.S., Reis e Sousa, C., Matsuura, Y., Fujita, T., Akira, S., 2006. Differential roles of MDA5 and RIG-I helicases in the recognition of RNA viruses. Nature 441, 101–105.

Kida, H., Yanagawa, R., Matsuoka, Y., 1980. Duck influenza lacking evidence of disease signs and immune response. Infect. Immun. 30, 547–553.

Li, H., Bradley, K.C., Long, J.S., Frise, R., Ashcroft, J.W., Hartgroves, L.C., Shelton, H., Makris, S., Johansson, C., Cao, B., Barclay, W.S., 2018. Internal genes of a highly pathogenic H5N1 influenza virus determine high viral replication in myeloid cells and severe outcome of infection in mice. PLoS Pathog. 14, e1006821.

Liang, Y., Danzy, S., Dao, L.D., Parslow, T.G., Liang, Y., 2012. Mutational analyses of the influenza A virus polymerase subunit PA reveal distinct functions related and unrelated to RNA polymerase activity. PLoS One 7, e29485.

Loo, Y.M., Fornek, J., Crochet, N., Bajwa, G., Perwitasari, O., Martinez-Sobrido, L., Akira, S., Gill, M.A., Garcia-Sastre, A., Katze, M.G., Gale Jr, M., 2008. Distinct RIG-I and MDA5 signaling by RNA viruses in innate immunity. J. Virol. 82, 335–345.

Marjuki, H., Scholtissek, C., Franks, J., Negovetich, N.J., Aldridge, J.R., Salomon, R., Finkelstein, D., Webster, R.G., 2010. Three amino acid changes in PB1-F2 of highly pathogenic H5N1 avian influenza virus affect pathogenicity in mallard ducks. Arch. Virol. 155, 925–934.

Maughan, M.N., Dougherty, L.S., Preskenis, L.A., Ladman, B.S., Gelb Jr, J., Spackman, E.V., Keeler Jr, C.L., 2013. Transcriptional analysis of the innate immune response of ducks to different species-of-origin low pathogenic H7 avian influenza viruses. Virol. J. 10, 94.

Miranzo-Navarro, D., Magor, K.E., 2014. Activation of duck RIG-I by TRIM25 is independent of anchored ubiquitin. PLoS One 9 e86968.

Mok, K.P., Wong, C.H.K., Cheung, C.Y., Chan, M.C., Lee, S.M.Y., Nicholls, J.M., Guan, Y., Peiris, J.S.M., 2009. Viral genetic determinants of H5N1 influenza viruses that contribute to cytokine dysregulation. J. Infect. Dis. 200, 1104–1112.

Pantin-Jackwood, M.J., Smith, D.M., Wasilenko, J.L., Cagle, C., Shepherd, E., Sarmento, L., Kapczynski, D.R., Afonso, C.L., 2012. Effect of age on the pathogenesis and innate immune responses in Pekin ducks infected with different H5N1 highly pathogenic avian influenza viruses. Virus Res. 167, 196–206.

Peisley, A., Wu, B., Xu, H., Chen, Z.J., Hur, S., 2014. Structural basis for ubiquitin-mediated antiviral signal activation by RIG-I. Nature 509, 110–114.

Reed, L.D., Muench, H., 1938. A simple method of estimating fifty percent endpoints. Am. J. Hyg. 27, 493–497.

Saito, L.B., Diaz-Satizabal, L., Evseev, D., Fleming-Canepa, X., Mao, S., Webster, R.G., Magor, K.E., 2018. IFN and cytokine responses in ducks to genetically similar H5N1 influenza A viruses of varying pathogenicity. J. Gen. Virol. 99, 464–474.

Sakabe, S., Takano, R., Nagamura-Inoue, T., Yamashita, N., Nidom, C.A., Quynh Le, M., Iwatsuki-Horimoto, K., Kawaoka, Y., 2013. Differences in cytokine production in human macrophages and in virulence in mice are attributable to the acidic polymerase protein of highly pathogenic influenza A virus subtype H5N1. J. Infect. Dis. 207, 262–271.

Salomon, R., Franks, J., Govorkova, E.A., Ilyushina, N.A., Yen, H.L., Hulse-Post, D.J., Humberd, J., Trichet, M., Rehg, J.E., Webby, R.J., Webster, R.G., Hoffmann, E., 2006. The polymerase complex genes contribute to the high virulence of the human H5N1 influenza virus isolate A/Vietnam/1203/04. J. Exp. Med. 203, 689–697.

Schoggins, J.W., Wilson, S.J., Panis, M., Murphy, M.Y., Jones, C.T., Bieniasz, P., Rice, C.M., 2011. A diverse range of gene products are effectors of the type I interferon antiviral response. Nature 472, 481–485.

Slemons, R.D., Easterday, B.C., 1978. Virus replication in the digestive tract of ducks exposed by aerosol to type-A influenza. Avian Dis. 22, 367–377.

Smith, J., Smith, N., Yu, L., Paton, I.R., Gutowska, M.W., Forrest, H.L., Danner, A.F., Seiler, J.P., Digard, P., Webster, R.G., Burt, D.W., 2015. A comparative analysis of host responses to avian influenza infection in ducks and chickens highlights a role for the interferon-induced transmembrane proteins in viral resistance. BMC Genomics 16, 574.

Sturm-Ramirez, K.M., Ellis, T., Bousfield, B., Bissett, L., Dyrting, K., Rehg, J.E., Poon, L., Guan, Y., Peiris, M., Webster, R.G., 2004. Reemerging H5N1 influenza viruses in Hong Kong in 2002 are highly pathogenic to ducks. J. Virol. 78, 4892–4901.

Sturm-Ramirez, K.M., Hulse-Post, D.J., Govorkova, E.A., Humberd, J., Seiler, P., Puthavathana, P., Buranathai, C., Nguyen, T.D., Chaisingh, A., Long, H.T., Naipospos, T.S., Chen, H., Ellis, T.M., Guan, Y., Peiris, J.S., Webster, R.G., 2005. Are ducks contributing to the endemicity of highly pathogenic H5N1 influenza virus in Asia? J. Virol. 79, 11269–11279.

Te Velthuis, A.J.W., Long, J.C., Bauer, D.L.V., Fan, R.L.Y., Yen, H.L., Sharps, J., Siegers, J.Y., Killip, M.J., French, H., Oliva-Martin, M.J., Randall, R.E., de Wit, E., van Riel, D., Poon, L.L.M., Fodor, E., 2018. Mini viral RNAs act as innate immune agonists during influenza virus infection. Nat. Microbiol. 3, 1234–1242.

Vanderven, H., Petkau, K., Ryan-Jean, K.E., Aldridge, J.R., Webster, R.G., Magor, K.E., 2012. Avian influenza rapidly induces antiviral genes in duck lung and intestine. Mol. Immunol. 51, 316–324.

Webster, R.G., Bean, W.J., Gorman, O.T., Chambers, T.M., Kawaoka, Y., 1992. Evolution and ecology of influenza A viruses. Microbiol. Rev. 56, 152–179.

Webster, R.G., Yakhno, M., Hinshaw, V.S., Bean, W.J., Murti, K.G., 1978. Intestinal influenza: replication and characterization of influenza viruses in ducks. Virology 84, 268–278.

Wei, L., Jiao, P., Song, Y., Cao, L., Yuan, R., Gong, L., Cui, J., Zhang, S., Qi, W., Yang, S., Liao, M., 2013. Host immune responses of ducks infected with H5N1 highly pathogenic avian influenza viruses of different pathogenicities. Vet. Microbiol. 166, 386–393.

Wu, B., Peisley, A., Tetrault, D., Li, Z., Egelman, E.H., Magor, K.E., Walz, T., Penczek, P.A., Hur, S., 2014. Molecular imprinting as a signal-activation mechanism of the viral RNA sensor RIG-I. Mol. Cell 55, 511–523.

Zeng, W., Sun, L., Jiang, X., Chen, X., Hou, F., Adhikari, A., Xu, M., Chen, Z.J., 2010. Reconstitution of the RIG-I pathway reveals a signaling role of unanchored polyubiquitin chains in innate immunity. Cell 141, 315–330.